EFFECT OF FIBER VOLUME FRACTION ON THE VARIATION OF STOCHASTIC ELASTIC CONSTANTS OF PLAIN-WEAVE COMPOSITE

Hao Wang[1], Xiu-wei Yu[2] and Zhong-wei Wang[3]

[1]Science and Technology on Scramjet Laboratory, National University of Defense Technology, Hunan, Changsha 410073, China. E-mail: gfkdwh@163.com
[2]Science and Technology on Scramjet Laboratory, National University of Defense Technology, Hunan, Changsha 410073, China. E-mail: yuxiuwei13@nudt.edu.cn
[3]Science and Technology on Scramjet Laboratory, National University of Defense Technology, Hunan, Changsha 410073, China. E-mail: wang_zhwei2001@163.com

Keywords: Textile composite, Fiber volume fraction, Mechanical properties, Computational modeling

ABSTRACT

Fiber volume fraction of yarn has obvious influence on the elastic constants of fiber yarn. In order to investigate the effect of fiber volume fraction of yarn on elastic constants of plain-weave composite, a new method to calculate the elastic constants of fiber yarn is established based on Local Stochastic Variable Metric Basis. A real yarn in the fabric composite has stochastic waviness, scaling and twist variations. Different values of fiber volume fraction are applied into three cases with the new method, and the effects of fiber volume fraction of yarn on elastic constants of plain-weave composites in three cases are acquired, respectively. As the fiber volume fraction of yarn increases, the impact bounds of elastic moduli of plain-weave composites decrease while the impact bounds of shear moduli increase. The variation trends of the impact bounds of Poisson's ratios are different in the three cases.

1 INTRODUCTION

Because of the high strength ratios and stiffness ratios, fiber reinforced composites are widely used in the area of aeronautics and astronautics, which decreases the weight of structures. Compare with the laminates, fabric composites have higher strength and stiffness and are replacing the use of laminates. During the producing process of composites, aleatoric uncertainties always exits in the microstructures of composites, which results in the scatter of mechanical properties of composites[1].

Many research teams have studied the methods to calculate the elastic constants of a real fiber yarn in textile composite[2, 3]. Gommer et al [4] used a method based on Hungary algorithm to reconstruct the path of fibers in yarn and this method can utilize traditional optical imaging technology to analysis the distribution of fiber in the yarn. The study suggests that the fibers of irregular directions in the yarn have impact on the mechanical properties (compliance and stiffness) of the yarn. For C/Fiber reinforced composites, the prediction of strength has 15% difference to the true value. Vanaerschot et al. [5-7] defined 6 parameters to fully describe each yarn path and cross-section shape in composites. Each parameter was decomposed into systematic value and a zero-mean stochastic deviation. Wang and Wang [8-10] established a local variable metric stochastic theory to quantify the influence of stochastic feature parameters of yarn on elastic properties of plain-weave composites. Taylor expansions of compliance of yarn were executed in global mean to estimate the local mean and standard deviation of elastic constants. Volumetric averaging method was employed to obtain the elastic constants of plain-weave composites.

Fiber yarns exit in the fabric composites, and the fiber volume fraction (FVF) of yarn has obvious effect on the elastic constants of yarn and composite[11]. Lee et al [12] proposed a geometric and elastic models based on the unit cell to predict the geometric characteristics and the elastic constants of plain-weave carbon fabric reinforced metal matrix composites. Increase of FVF entails the higher angle of yarn crimp, which in turn increases off-axis angle of yarns, resulting in the reduced moduli of woven composites. Tsai et al [13] proposed a parallelogram spring model to investigate the effects of fabric parameters on the elastic moduli of braided composite plates. The simulation results of FEM show that all the Young's moduli increase almost linearly with the increase of FVF.

The focus of this paper is to study the effect of yarn FVF on elastic constants of plain-weave composites. Firstly, local stochastic variable metric theory is established to transform a real yarn into a ideal yarn, and estimate the elastic constants of real yarns. Then, the volumetric averaging method is performed to acquire the elastic constants of plain-weave composite. At last, three values of yarn FVF are applied into the estimation of elastic constants of plain-weave composites. The influence of yarn FVF on elastic constants of plain-weave composites is acquired by comparing the simulation results.

2 FEATURE PARAMETERS OF YARN

A global coordinate system with orthogonal axes 1-2-3 is defined to describe the yarn of plain-weave composites, where 1-axis is along the longitudinal direction of yarn. A real yarn in the fabric composite can be fully characterized by 6 feature parameters, namely path vector $\boldsymbol{r}$ (x_1, x_2, x_3) and geometric parameters (a, b, θ) (see Fig. 1).

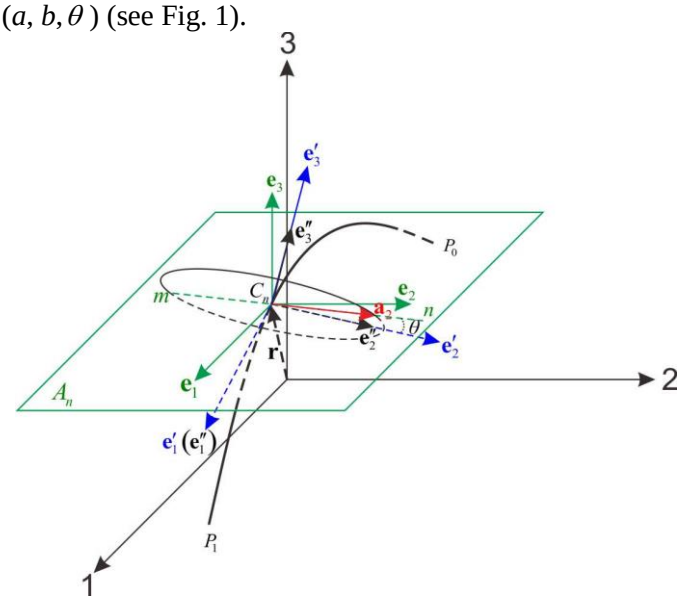

Fig. 1 The feature parameters of yarn (i.e. path vector r ,scaling matrix $\hat{\partial}''$ and twist angle θ), and the global $\{\boldsymbol{e}_1,\boldsymbol{e}_2,\boldsymbol{e}_3\}$, local $\{\boldsymbol{e}_1',\boldsymbol{e}_2',\boldsymbol{e}_3'\}$ and variable metric basic $\{\boldsymbol{e}_1'',\boldsymbol{e}_2'',\boldsymbol{e}_3''\}$ [9]

Ellipse is used to describe the cross-section shape of yarn and the parameters a and b are the semi-major and semi-minor axes of elliptic cross-section. θ is the orientation of yarn's cross-section, which describes the twist extent of yarn around the tangent vector of the yarn path. The path vector describes the yarn waviness and deflection, while the geometric parameters represent the shape and orientation of the yarn cross-section.

For arbitrary position of yarn center path C_n in Fig. 2, $\boldsymbol{r}$ is the vector from original point to point C_n.

$$\mathbf{r}(\xi)=x_i(\xi)\mathbf{e}_i \tag{1}$$

where $\mathbf{e}_i\ (i=1,2,3)$ are the basis of global system, and $x_1(\xi)=\xi$.

A local coordinate system 1'-2'-3' at arbitrary position of yarn path is defined in Fig. 1, where 1'-axis is in the direction of tangent vector of yarn path, 2'- and 3'-axes are in the direction of semi-major and semi-minor axes of yarn cross-section, respectively. A variable metric coordinate system 1"-2"-3" overlapped with the defined local coordinate system is defined, but the metric between them is different along each of the same axis direction. Correspondingly, three triads of unit bases $\{\mathbf{e}_1,\mathbf{e}_2,\mathbf{e}_3\}$, $\{\mathbf{e}_1',\mathbf{e}_2',\mathbf{e}_3'\}$ and $\{\mathbf{e}_1'',\mathbf{e}_2'',\mathbf{e}_3''\}$ corresponding to the global, local and variable metric coordinate system are created.

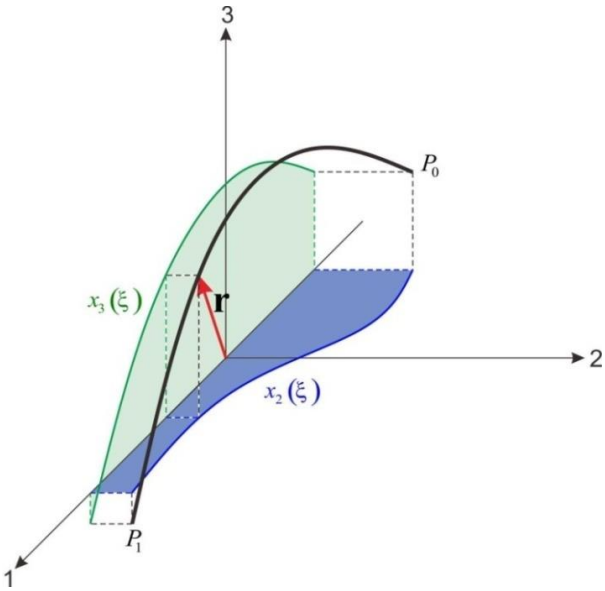

Fig. 2 The orthogonal decomposition of path vector in 1–2 and 1–3 planes.

Obviously, the relationship between global and local coordinate system is expressed by a rotation transformation, thus the following tensor expression is obtained.

$$v_i = v'_j e'_{ji} \tag{2}$$

where v_i, v'_j are the components of vector in global and local coordinate system, respectively, and $e'_{ji} = e'_j \bullet e_i$ is rotation transformation matrix where symbol "$\bullet$" denotes scalar (dot) product.

Because of different metrics between local and variable metric coordinate system, the components of vector in the two coordinate systems are not the same. Let v''_i denotes the components of vector in variable metric coordinate system. The transformation relationship between the two coordinate systems is defined as below.

$$v'_i = \vartheta''_{ij} v''_j = v''_j \vartheta''_{ji} \tag{3}$$

where ϑ''_{ij} are second order symmetric tensors, named scaling tensor and $\vartheta''_{ij} = 0$ when $i \neq j$. Due to that ϑ''_{ij} is a diagonal matrix, $\vartheta''_{ij} = \vartheta''_{ji}$. It is usually represented variable metric transformation Eq. (3) in entity form by

$$\mathbf{v}' = \hat{\boldsymbol{\vartheta}}'' \bullet \mathbf{v}'' = \mathbf{v}'' \bullet \hat{\boldsymbol{\vartheta}}'' \tag{4}$$

Substitute Eq. (3) into Eq. (2), one can obtain the following transformation rules between global and variable metric coordinate system.

$$v_i = v'_j e'_{ji} = v''_k \vartheta''_{kj} e'_{ji} = v''_k \kappa''_{ki} \tag{5}$$

$$\mathbf{v} = \mathbf{v}'' \bullet \hat{\boldsymbol{\vartheta}}'' \bullet \hat{\mathbf{e}}' = \mathbf{v}'' \bullet \hat{\boldsymbol{\kappa}}'' \tag{6}$$

where $\hat{\boldsymbol{\kappa}}'' = \hat{\boldsymbol{\vartheta}}'' \bullet \hat{\mathbf{e}}'$ is variable metric coordinate transformation matrix.

Each feature parameter can be decomposed as

$$\rho = \langle \rho \rangle + \overset{\circ}{\rho}, \quad \rho = x_2, x_3, a, b, \theta \tag{7}$$

where $\langle \rho \rangle$ is the systematic value and $\overset{\circ}{\rho}$ is zero-mean deviation from the systematic value.

The global values of *a* and *b* are obtained by integrating along the yarn path.

$$\tilde{a} = \frac{1}{L} \int_{\mathbf{r}} \langle a(\xi) \rangle \mathrm{d}L, \qquad \tilde{b} = \frac{1}{L} \int_{\mathbf{r}} \langle b(\xi) \rangle \mathrm{d}L \tag{8}$$

where $\mathrm{d}L = \sqrt{\dot{\mathbf{r}} \bullet \dot{\mathbf{r}}} \mathrm{d}\xi$.

In the variable metric coordinate, $\hat{\boldsymbol{\vartheta}}''$ can be defined as

$$\begin{aligned}\hat{\vartheta}''(\xi) &= \operatorname{diag}\left\{\vartheta''_{11}(\xi), \vartheta''_{22}(\xi), \vartheta''_{33}(\xi)\right\} = \operatorname{diag}\left\{1, \frac{a(\xi)}{\tilde{a}}, \frac{b(\xi)}{\tilde{b}}\right\} \\ &= \operatorname{diag}\left\{1, \frac{\langle a(\xi)\rangle + \overset{\circ}{a}(\xi)}{\tilde{a}}, \frac{\langle b(\xi)\rangle + \overset{\circ}{b}(\xi)}{\tilde{b}}\right\} \\ &= \operatorname{diag}\left\{1, \langle \vartheta''_{22}\rangle + \overset{\circ}{\vartheta}''_{22}, \langle \vartheta''_{33}\rangle + \overset{\circ}{\vartheta}''_{33}\right\}\end{aligned} \tag{9}$$

where $\vartheta''_{11}(\xi) \equiv 1$ represents the scaling factor in 1-axis.

3 EXPANSION OF LOCAL STOCHASTIC VARIABLE METRIC BASIS(LSVMB)

3.1 CALCULATION OF LOCAL BASIS

The tangent vector of the yarn path is defined as

$$\mathbf{e}'_1 = \frac{\dot{\mathbf{r}}(\xi)}{|\dot{\mathbf{r}}(\xi)|} \tag{10}$$

In Fig. 1, the yarn cross-section at path point C_n and plane A_n intersect in a unit vector $\mathbf{a}_2$, and $\mathbf{a}_2$ has the following relation with constant vector e_3.

$$\mathbf{a}_2 = \frac{\mathbf{e}_3 \times \mathbf{e}'_1}{|\mathbf{e}_3 \times \mathbf{e}'_1|} = \frac{\mathbf{e}_3 \times \dot{\mathbf{r}}}{|\mathbf{e}_3 \times \dot{\mathbf{r}}|} \tag{11}$$

With the introduction of Rodrigues' rotation formula into $\mathbf{a}_2$ about $\mathbf{e}'_1$, the unit vectors $\mathbf{e}'_2$ and $\mathbf{e}'_3$ can be evaluated as

$$\begin{aligned}\mathbf{e}'_2 &= \frac{(\mathbf{e}_3 \times \mathbf{e}'_1)\cos\theta + \left[\mathbf{e}_3 - (\mathbf{e}'_1 \bullet \mathbf{e}_3)\mathbf{e}'_1\right]\sin\theta}{|\mathbf{e}_3 \times \mathbf{e}'_1|} \\ \mathbf{e}'_3 &= \frac{\left[\mathbf{e}_3 - (\mathbf{e}'_1 \bullet \mathbf{e}_3)\mathbf{e}'_1\right]\cos\theta - (\mathbf{e}_3 \times \mathbf{e}'_1)\sin\theta}{|\mathbf{e}_3 \times \mathbf{e}'_1|}\end{aligned} \tag{12}$$

3.2 COVARIANCES OF FEATURE PARAMETERS

Corresponding to the components of feature parameters, the covariances of feature parameters are decomposed into three parts, namely tangent vectors, scaling matrix and twist angle. Since the covariance function is 2nd centered moment, the covariance function is closely related to the standard deviation of each feature parameter

(1) In stochastic waviness case, the covariance function of tangent vector is defined as (warp genus)

$$\hat{\mathbf{K}}_{\dot{\mathbf{r}}\dot{\mathbf{r}}} = \operatorname{diag}\left\{0, K_{\dot{x}_2\dot{x}_2}, K_{\dot{x}_3\dot{x}_3}\right\} = K_{\dot{x}_i\dot{x}_j}\mathbf{e}_i \otimes \mathbf{e}_j \tag{13}$$

where $K_{\dot{x}_i\dot{x}_i} = \left\langle \overset{\circ}{\dot{x}}_i \overset{\circ}{\dot{x}}_i \right\rangle = \left\langle \tan^2\alpha_i \right\rangle \approx \sigma^2_{\alpha_i}$, σ_{α_i} is standard deviation of the deflection angle α which is defined as the angle between the direction of the perfect yarn path and local tangent to the realization of the stochastic yarn path, and the symbol ‘‘$\otimes$’’ denotes outer tensor product.

(2) In stochastic twist case, the covariance function of twist angle θ is defined as

$$K_{\theta\theta}(\xi,\xi) = \left\langle \overset{\circ}{\theta}(\xi)\overset{\circ}{\theta}(\xi) \right\rangle = \sigma^2_\theta \tag{14}$$

with σ_θ the standard deviation θ.

(3) In stochastic scaling case, the covariance of scaling matrix [9] is defined as

$$\mathbf{K}_{\hat{\vartheta}''\hat{\vartheta}''} = \left\langle \overset{\circ}{\hat{\vartheta}}'' \otimes \overset{\circ}{\hat{\vartheta}}'' \right\rangle = K_{\vartheta''_{ij}\vartheta''_{mn}}\mathbf{e}_i \otimes \mathbf{e}_j \otimes \mathbf{e}_m \otimes \mathbf{e}_n \tag{15}$$

where $K_{\vartheta''_{22}\vartheta''_{22}} = \left\langle \overset{\circ}{\vartheta}''_{22}\overset{\circ}{\vartheta}''_{22} \right\rangle = \dfrac{\left\langle \overset{\circ}{a}\overset{\circ}{a} \right\rangle}{\tilde{a}^2} = \left(\dfrac{\sigma_a}{\tilde{a}}\right)^2 = c_{v_a}^2$, $K_{\vartheta''_{33}\vartheta''_{33}} = \left\langle \overset{\circ}{\vartheta}''_{33}\overset{\circ}{\vartheta}''_{33} \right\rangle = \dfrac{\left\langle \overset{\circ}{b}\overset{\circ}{b} \right\rangle}{\tilde{b}^2} = \left(\dfrac{\sigma_b}{\tilde{b}}\right)^2 = c_{v_b}^2$.

3.3 EXPANSION OF LSVMB

The LSVMB of the path are defined as

$$\begin{aligned}
\boldsymbol{\kappa}''_1 &= \hat{\boldsymbol{\vartheta}}''\bullet\dot{\mathbf{r}}' = \frac{\hat{\boldsymbol{\vartheta}}''\bullet\dot{\mathbf{r}}}{|\dot{\mathbf{r}}|} \\
\boldsymbol{\kappa}''_2 &= \hat{\boldsymbol{\vartheta}}''\bullet\mathbf{e}'_2 = \frac{\hat{\boldsymbol{\vartheta}}''\bullet(\mathbf{e}_3\times\mathbf{e}'_1)\cos\theta + \hat{\boldsymbol{\vartheta}}''\bullet\mathbf{e}_3\sin\theta - (\mathbf{e}'_1\bullet\mathbf{e}_3)\hat{\boldsymbol{\vartheta}}''\bullet\mathbf{e}'_1\sin\theta}{|\mathbf{e}_3\times\mathbf{e}'_1|} \\
\boldsymbol{\kappa}''_3 &= \hat{\boldsymbol{\vartheta}}''\bullet\mathbf{e}'_3 = \frac{\hat{\boldsymbol{\vartheta}}''\bullet\mathbf{e}_3\cos\theta - (\mathbf{e}'_1\bullet\mathbf{e}_3)\hat{\boldsymbol{\vartheta}}''\bullet\mathbf{e}'_1\cos\theta - \hat{\boldsymbol{\vartheta}}''\bullet(\mathbf{e}_3\times\mathbf{e}'_1)\sin\theta}{|\mathbf{e}_3\times\mathbf{e}'_1|}
\end{aligned} \tag{16}$$

Because $\mathbf{e}'_1,\mathbf{e}'_2,\mathbf{e}'_3$ are mutually orthogonal and scaling tensor $\hat{\boldsymbol{\vartheta}}''$ does not affect the direction of local basis, the LSVMB $\boldsymbol{\kappa}''_1,\boldsymbol{\kappa}''_2,\boldsymbol{\kappa}''_3$ are mutually orthogonal. Eq.(16) shows the LSVMB are the function of 1st derivative of path vector, scaling matrix and twist angle. Expansion of the LSVMB $\boldsymbol{\kappa}''_1,\boldsymbol{\kappa}''_2,\boldsymbol{\kappa}''_3$ into Taylor's series about the mean parameters $\dot{\mathbf{r}} = \langle\dot{\mathbf{r}}\rangle$, $\hat{\boldsymbol{\vartheta}}'' = \langle\hat{\boldsymbol{\vartheta}}''\rangle$, $\theta = \langle\theta\rangle$ yields:

$$\boldsymbol{\kappa}''_i = \mathbf{a}^{(i)} + \hat{\mathbf{b}}^{(i)}\bullet\overset{\circ}{\dot{\mathbf{r}}} + \hat{\mathbf{c}}^{(i)} : \overset{\circ}{\hat{\boldsymbol{\vartheta}}}'' + \mathbf{d}^{(i)}\overset{\circ}{\theta} + \frac{1}{2}\left[\hat{\mathbf{f}}^{(i)} : \overset{\circ}{\dot{\mathbf{r}}}\otimes\overset{\circ}{\dot{\mathbf{r}}} + \mathbf{t}^{(i)}\bullet\left(\overset{\circ}{\theta}\cdot\overset{\circ}{\theta}\right)\right] + \cdots\cdots \tag{17}$$

where $\mathbf{a}^{(i)} = \boldsymbol{\kappa}''_i\big|_{\Omega=\langle\Omega\rangle}$, $\hat{\mathbf{b}}^{(i)} = \dfrac{\partial\boldsymbol{\kappa}''_i}{\partial\dot{\mathbf{r}}}\Big|_{\Omega=\langle\Omega\rangle}$, $\hat{\mathbf{c}}^{(i)} = \dfrac{\partial\boldsymbol{\kappa}''_i}{\partial\hat{\boldsymbol{\vartheta}}''}\Big|_{\Omega=\langle\Omega\rangle}$, $\mathbf{d}^{(i)} = \dfrac{\partial\boldsymbol{\kappa}''_i}{\partial\theta}\Big|_{\Omega=\langle\Omega\rangle}$, $\hat{\mathbf{f}}^{(i)} = \dfrac{\partial^2\boldsymbol{\kappa}''_i}{\partial\dot{\mathbf{r}}\partial\dot{\mathbf{r}}}\Big|_{\Omega=\langle\Omega\rangle}$, $\mathbf{t}^{(i)} = \dfrac{\partial^2\boldsymbol{\kappa}''_i}{\partial\theta\partial\theta}\Big|_{\Omega=\langle\Omega\rangle}$, $\Omega = \dot{\mathbf{r}},\hat{\boldsymbol{\vartheta}}'',\theta$. In Eq. (17), $\mathbf{a}^{(i)}$ represents the elastic constants of ideal yarn, $\hat{\mathbf{b}}^{(i)},\hat{\mathbf{f}}^{(i)}$ represents the stochastic waviness of yarn path, $\hat{\mathbf{c}}^{(i)}$ represents the stochastic scaling of yarn cross-section, and $\mathbf{d}^{(i)},\mathbf{t}^{(i)}$ represents the twist of yarn.

The 2nd approximation of the mean of LSVMB is

$$\langle\boldsymbol{\kappa}''_i\rangle = \mathbf{a}^{(i)} + \frac{1}{2}\left[\hat{\mathbf{f}}^{(i)} : \hat{\mathbf{K}}_{\dot{\mathbf{r}}\dot{\mathbf{r}}} + \mathbf{t}^{(i)}\bullet K_{\theta\theta}\right] \tag{18}$$

The waviness of $\boldsymbol{\kappa}''_i$ relative to $\langle\boldsymbol{\kappa}''_i\rangle$ is

$$\overset{\circ}{\boldsymbol{\kappa}}''_i = \hat{\mathbf{b}}^{(i)}\bullet\overset{\circ}{\dot{\mathbf{r}}} + \hat{\mathbf{c}}^{(i)} : \overset{\circ}{\hat{\boldsymbol{\vartheta}}}'' + \mathbf{d}^{(i)}\overset{\circ}{\theta} \tag{19}$$

Thus, the 1st order approximation of the covariance of LSVMB is obtained as following

$$\left\langle \overset{\circ}{\boldsymbol{\kappa}}''_i\otimes\overset{\circ}{\boldsymbol{\kappa}}''_j \right\rangle = \hat{\mathbf{b}}^{(i)}\bullet\hat{\mathbf{K}}_{\dot{\mathbf{r}}\dot{\mathbf{r}}}\bullet\left(\hat{\mathbf{b}}^{(j)}\right)^T + \hat{\mathbf{c}}^{(i)} : \mathbf{K}_{\hat{\boldsymbol{\vartheta}}''\hat{\boldsymbol{\vartheta}}''} : \left(\hat{\mathbf{c}}^{(j)}\right)^o + K_{\theta\theta}\mathbf{d}^{(i)}\otimes\mathbf{d}^{(j)} \tag{20}$$

where the superscripts "T" represents the transposition of 3rd order tensor, and superscripts "o" represents the transposition rule $\left(\hat{\mathbf{c}}^{(j)}\right)^o = c_{ijk}^{(j)}\mathbf{e}_j\otimes\mathbf{e}_k\otimes\mathbf{e}_i$.

For the purpose of convenience, the nine-component vector of variable metric directional cosines are introduced as follows

$$\boldsymbol{\kappa}'' = \{\boldsymbol{\kappa}''_1,\boldsymbol{\kappa}''_2,\boldsymbol{\kappa}''_3\} = \{\kappa''_{11},\kappa''_{12},\kappa''_{13},\kappa''_{21},\kappa''_{22},\kappa''_{23},\kappa''_{31},\kappa''_{32},\kappa''_{33}\} \tag{21}$$

where $\kappa''_{ij} = \vartheta''_{ir}e'_{rj}$. Then, the covariance $\hat{\mathbf{K}}_{\boldsymbol{\kappa}''\boldsymbol{\kappa}''}$ of the LSVMB vectors can be written in the matrix form

$$\hat{\mathbf{K}}_{\boldsymbol{\kappa}''\boldsymbol{\kappa}''}=\left\langle \overset{\circ}{\boldsymbol{\kappa}}''\otimes\overset{\circ}{\boldsymbol{\kappa}}''\right\rangle=\begin{bmatrix}\left\langle \overset{\circ}{\boldsymbol{\kappa}}_1''\otimes\overset{\circ}{\boldsymbol{\kappa}}_1''\right\rangle & \left\langle \overset{\circ}{\boldsymbol{\kappa}}_1''\otimes\overset{\circ}{\boldsymbol{\kappa}}_2''\right\rangle & \left\langle \overset{\circ}{\boldsymbol{\kappa}}_1''\otimes\overset{\circ}{\boldsymbol{\kappa}}_3''\right\rangle \\ & \left\langle \overset{\circ}{\boldsymbol{\kappa}}_2''\otimes\overset{\circ}{\boldsymbol{\kappa}}_2''\right\rangle & \left\langle \overset{\circ}{\boldsymbol{\kappa}}_2''\otimes\overset{\circ}{\boldsymbol{\kappa}}_3''\right\rangle \\ symm & & \left\langle \overset{\circ}{\boldsymbol{\kappa}}_3''\otimes\overset{\circ}{\boldsymbol{\kappa}}_3''\right\rangle\end{bmatrix} \tag{22}$$

The local variable metric compliance or stiffness tensor $\mathfrak{R}''\left(\mathfrak{R}=\mathbf{C},\mathbf{S}\right)$ are related to the global compliance tensor $\mathfrak{R}$ through the following tensor transformation law.

$$\mathfrak{R}_{ijkl}=\mathfrak{R}''_{mnop}\vartheta''_{mr}e'_{ri}\vartheta''_{ns}e'_{sj}\vartheta''_{ot}e'_{tk}\vartheta''_{pu}e'_{ul}=\mathfrak{R}''_{mnop}\kappa''_{mi}\kappa''_{nj}\kappa''_{ok}\kappa''_{pl} \tag{23}$$

The mean compliance or stiffness of yarn [8, 9] can be obtained by

$$\left\langle\mathfrak{R}\right\rangle=\mathfrak{R}\big|_{\boldsymbol{\kappa}''=\left\langle\boldsymbol{\kappa}''\right\rangle}+\frac{1}{2}\hat{\mathbf{u}}^{(\mathfrak{R})}:\hat{\mathbf{K}}_{\boldsymbol{\kappa}''\boldsymbol{\kappa}''} \tag{24}$$

4 ELASTIC CONSTATNS OF PLAIN-WEAVE COMPOSITE

The volumes of warp and weft genuses are identical, hence the volume fraction of each yarn genus is 0.5. The formulations of $\hat{\mathfrak{R}}$ of plain-weave composite are acquired by applying volumetric averaging method to the compliance or stiffness of all genuses of materials [8].

$$\left\langle\hat{\mathfrak{R}}^{(aver)}\right\rangle=\frac{V_y}{2\left\langle L\right\rangle}\int\left(\left\langle\hat{\mathfrak{R}}^{(\mathrm{I})}\right\rangle+\left\langle\hat{\mathfrak{R}}^{(\mathrm{II})}\right\rangle\right)\mathrm{d}\left\langle L\right\rangle+V_m\hat{\mathfrak{R}}^{(m)} \tag{25}$$

where the superscripts “(I)”, “(II)” and “(m)” represent warp, weft and matrix genuses, respectively. L represents the length of a yarn period. $V_m=1-V_y$ denotes the volume fraction of matrix in composite and V_y is the volume fraction of yarn in composite. Isostress method is conducted when $\hat{\mathfrak{R}}$ is compliance tensor, while the isostrain method is conducted when $\hat{\mathfrak{R}}$ is stiffness tensor[14]. The relations between elastic constants and compliance tensor[11] are

$$\begin{aligned}&S_{11}=\frac{1}{E_{11}},\quad S_{12}=-\frac{\nu_{12}}{E_{11}},\quad S_{13}=-\frac{\nu_{13}}{E_{11}}\\&S_{22}=\frac{1}{E_{22}},\quad S_{23}=-\frac{\nu_{23}}{E_{22}},\quad S_{33}=\frac{1}{E_{33}}\\&S_{44}=\frac{1}{G_{23}},\quad S_{55}=\frac{1}{G_{13}},\quad S_{66}=\frac{1}{G_{12}}\end{aligned} \tag{26}$$

5 RESULTS AND DISCUSSIONS

The impact bounds of elastic constants of plain-weave composite changes when the FVF of yarn changes. In order to study the effect of FVF on the elastic constants of plain-weave composites, three values of FVF are applied into the three cases of stochastic waviness, scaling and twist. The parameters of mechanical properties and FVF of yarn in plain-weave composites are listed in Table 1. The isostress and isostrain results corresponds to the upper and lower impact bounds of elastic constants. The results of elastic characteristics are expressed as the ratios of the mean elastic constants to the ideal ones (called impact bounds), which reflect the relative changes between the mean elastic constants and ideal ones with considering stochastic fluctuations in the feature parameters of yarn.

Table 1 Parameters of mechanical properties and fiber volume fraction of yarn in plain-weave composite

Parameters of composites		Parameter values
Elastic constants of composite constitutes	$E_{f11}\left(\mathrm{GPa}\right)$	200
	$E_{f22}\left(\mathrm{GPa}\right)$	100
	$G_{f12}\left(\mathrm{GPa}\right)$	50

	G_{f23} (GPa)	50
	ν_{f12}	0.3
	E_m (GPa)	100
	G_m (GPa)	50
	ν_m	0.3
Fiber volume fraction of composite constitutes	V_f	0.5 , 0.7 , 0.9
	V_y	0.7

5.1 STOCHASTIC WAVINESS

The influence of FVF on elastic constants of plain-weave composites in stochastic waviness case is shown in Fig. 3, and the solid and dashed line surfaces represent the results of isostress and isostrain methods, respectively.

The upper and lower impact bounds of elastic moduli exchange as σ_{α_y} increase when $\sigma_{\alpha_z} < 5°$. When FVF increase from 0.5 to 0.9, the both impact bounds of in-plane elastic moduli $\langle E_{11} \rangle$ and $\langle E_{22} \rangle$ show decreasing trends. The isostress impact bounds of out-of-plane elastic modulus $\langle E_{33} \rangle$ shows a slight increasing trend when $\sigma_{\alpha_y} > 5\sigma_{\alpha_z}$ and a decreasing trend in the other side.

As for in-plane shear modulus $\langle G_{12} \rangle$, the impact bounds of isostress and isostrain methods exchange as σ_{α_z} increases while σ_{α_y} is small. Similarly, the upper and lower impact bounds of out-of-plane shear modulus $\langle G_{13} \rangle$ and $\langle G_{23} \rangle$ exchange as σ_{α_y} increases while σ_{α_z} is small. When FVF increases from 0.5 to 0.9, the both impact bounds of shear moduli increase.

Similar to shear moduli, as for in-plane Poisson's ratio $\langle \nu_{12} \rangle$, the impact bounds of isostress and isostrain methods exchange as σ_{α_z} increases when σ_{α_y} is small. The impact bounds of out-of-plane Poisson's ratios $\langle \nu_{13} \rangle$ and $\langle \nu_{23} \rangle$ exchange as σ_{α_y} increases when σ_{α_z} is small. When FVF increases from 0.5 to 0.9, the both impact bounds of in-plane Poisson's ratios $\langle \nu_{12} \rangle$ decrease when $\sigma_{\alpha_z} > 6\sigma_{\alpha_y}$ and increase in the other side. Meanwhile, the isostress impact bounds of out-of-plane Poisson's ratios $\langle \nu_{13} \rangle$ and $\langle \nu_{23} \rangle$ change little when $\sigma_{\alpha_z} < 0.6\sigma_{\alpha_y}$ and increase slightly in the other side. The isostrain impact bounds decrease when $\sigma_{\alpha_z} < \sigma_{\alpha_y}$ and increase in the other side.

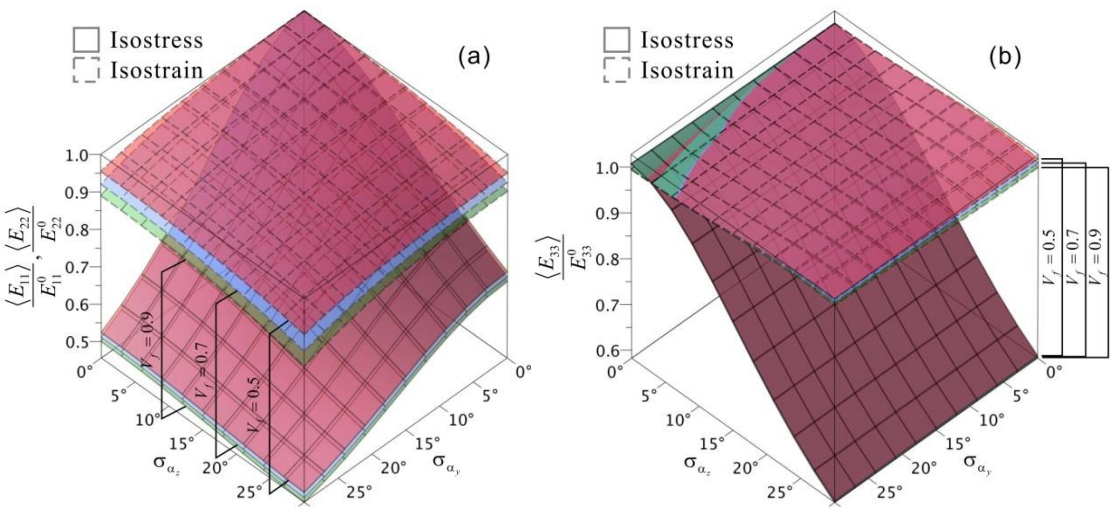

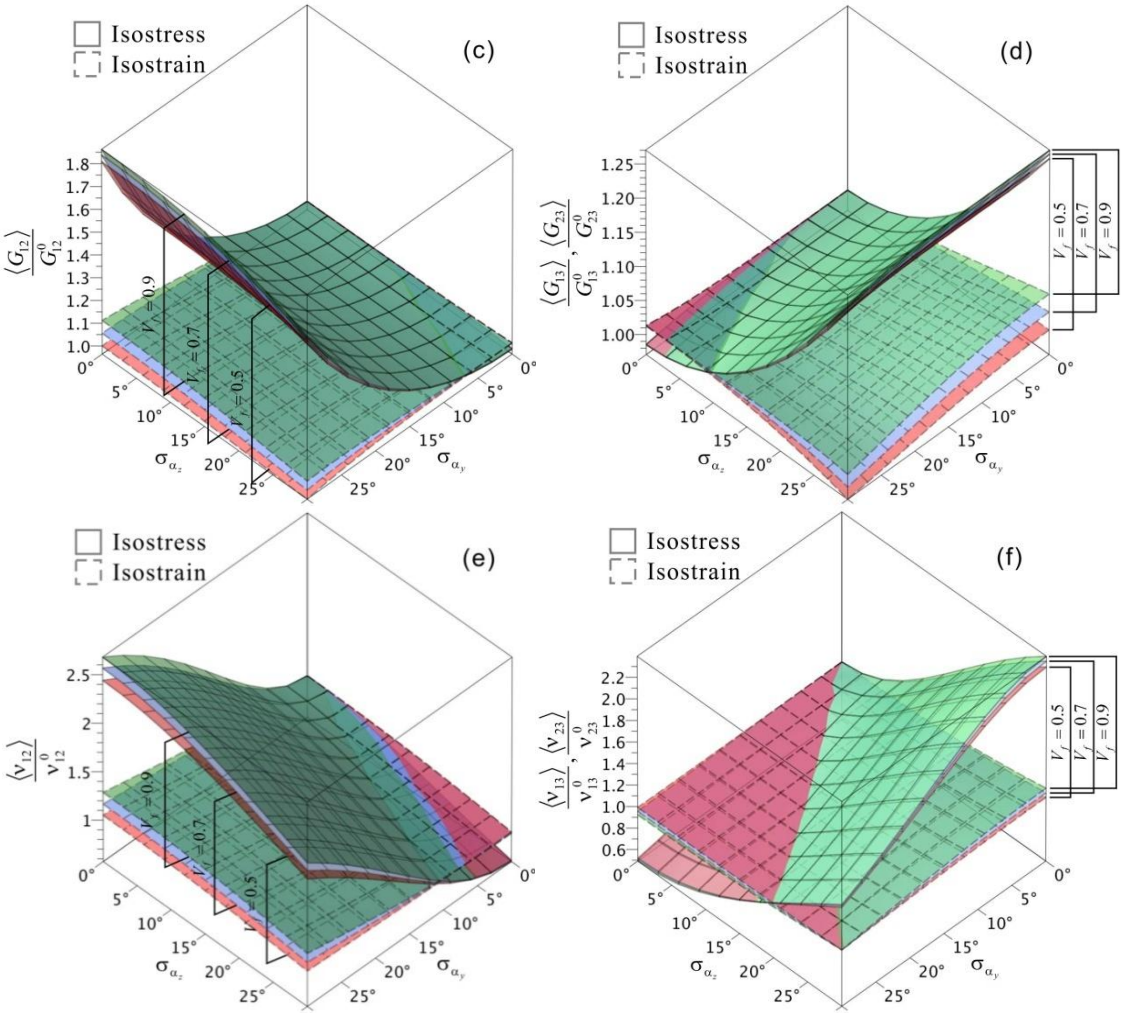

Fig. 3 The influence of V_f on elastic constants of plain-weave composites in stochastic waviness cases

5.2 STOCHASTIC SCALING

The influence of FVF on elastic constants of plain-weave composites in stochastic scaling case is shown in Fig. 4, and the solid and dashed line surfaces represent the results of isostress and isostrain methods, respectively.

When FVF increases from 0.5 to 0.9, the impact bounds of in-plane elastic modulus $\langle E_{11} \rangle$ and $\langle E_{22} \rangle$ decrease. Comparing with the upper impact bounds, the lower impact bounds are less sensitive to the variation of FVF. Meanwhile, the variation of FVF has no influence on the both impact bounds of $\langle E_{33} \rangle$. The influence of FVF on the both impact bounds of shear moduli is ignorable.

As FVF increases from 0.5 to 0.9, the influence of FVF on impact bounds of $\langle \nu_{12} \rangle$ becomes more and more significant as c_{v_a} increases. The both impact bounds of $\langle \nu_{13} \rangle$ and $\langle \nu_{23} \rangle$ exchange when $c_{v_a} = c_{v_b}$. The effects of FVF on impact bounds of $\langle \nu_{13} \rangle$ and $\langle \nu_{23} \rangle$ are not obvious. On the contrary, the impacts of FVF on the impact bounds of $\langle E_{11} \rangle$, $\langle E_{22} \rangle$ and $\langle \nu_{12} \rangle$ of plain-weave composites in stochastic scaling case are obvious.

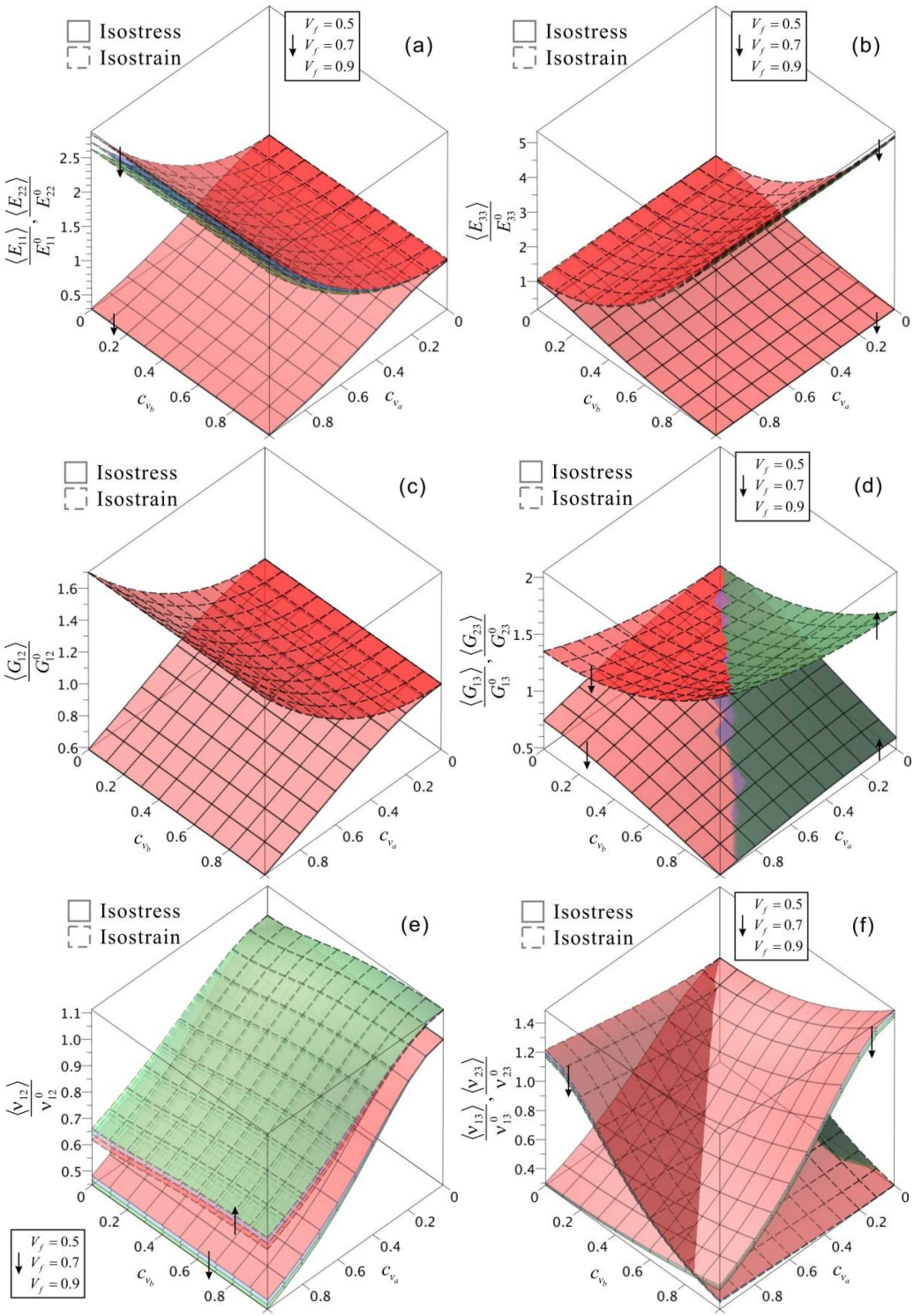

Fig. 4 The influence of V_f on elastic constants of plain-weave composites in stochastic scaling cases

5.3 STOCHASTIC TWIST

The influence of FVF on elastic constants of plain-weave composites in stochastic twist case is shown in Fig. 5, and the solid and dashed line surfaces represent the results of isostress and isostrain methods, respectively.

The impact bounds of in-plane elastic modulus $\langle E_{11}\rangle$ and $\langle E_{22}\rangle$ expand as FVF increase from 0.5 to 0.9. Isostress impact bounds of $\langle E_{11}\rangle$ and $\langle E_{22}\rangle$ are more sensitive to the variation of FVF than

isostrain impact bounds. Meanwhile, FVF has almost no impacts on the both impact bounds of out-of-plane elastic moduli $\langle E_{33} \rangle$.

The impact of FVF on the both impact bounds of shear moduli is not obvious. The isostress and isostrain impact bounds of shear moduli of plain-weave composites exchanges when $\sigma_\theta \approx 12° \sim 18°$.

When FVF increases from 0.5 to 0.9, the isostress impact bound of in-plane Poisson's ratio $\langle \nu_{12} \rangle$ decreases while those of out-of-plane Poisson's ratios $\langle \nu_{13} \rangle$ and $\langle \nu_{23} \rangle$ increase. Besides, the isostrain impact bounds of Poisson's ratios are almost not affected by the variation of FVF.

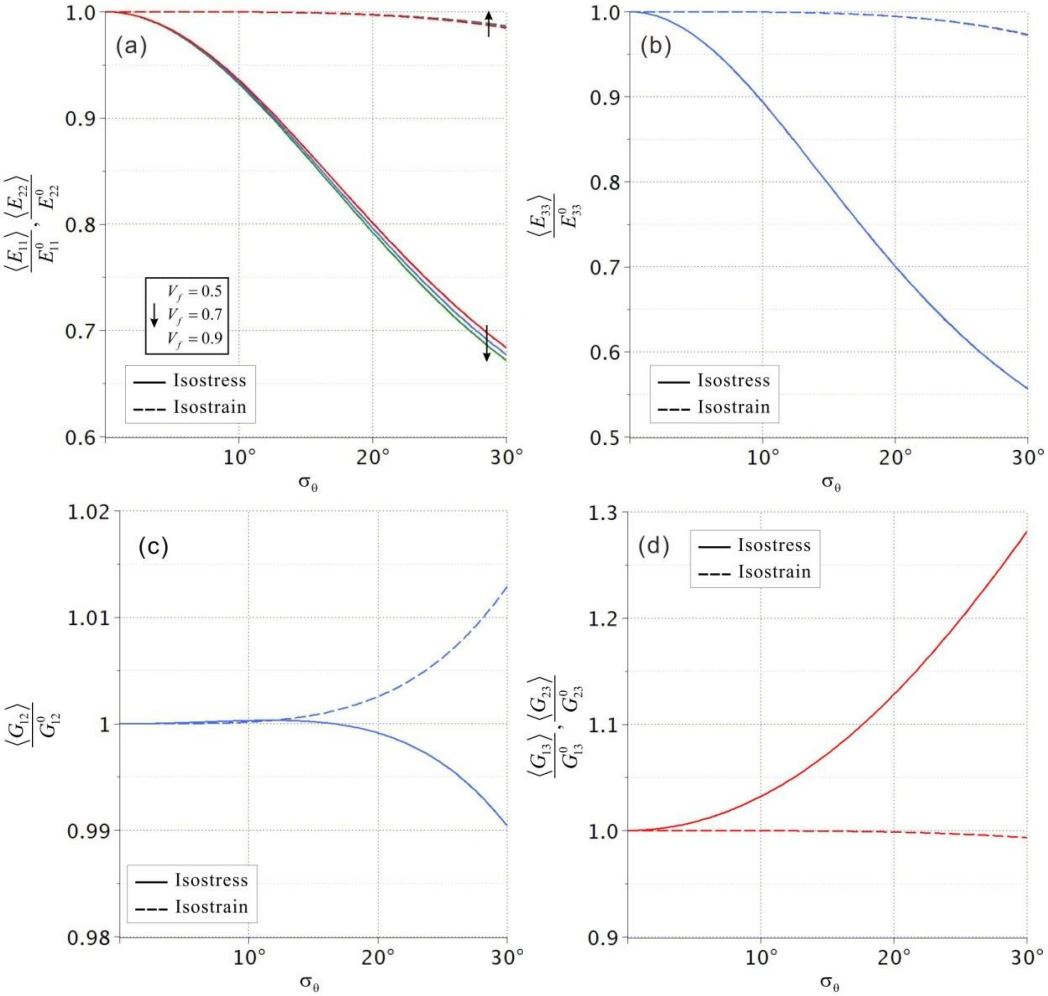

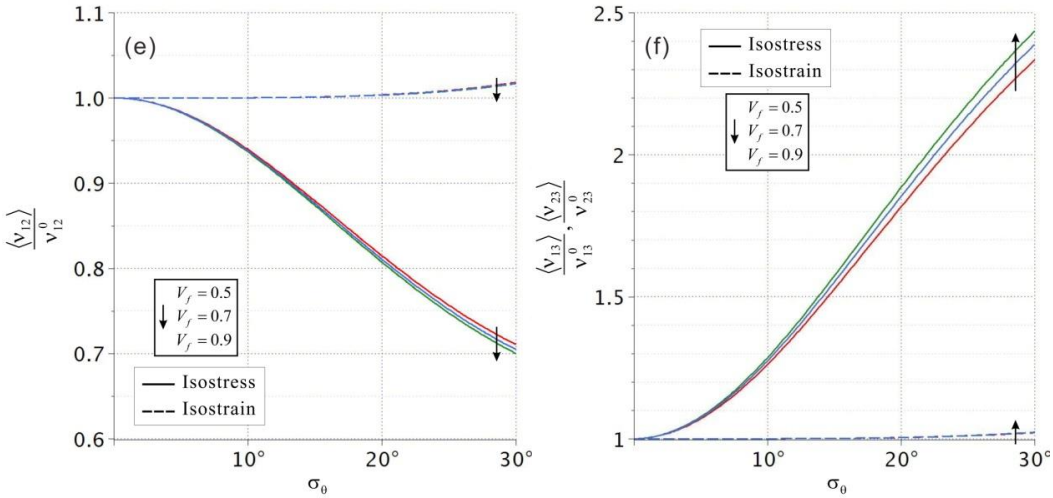

Fig. 5 The influence of V_f on elastic constants of plain-weave composites in stochastic twist cases

6 CONCLUSIONS

A real yarn can be transformed into a ideal yarn by LSVMB. This paper presents a new method to estimate the elastic constants of fiber yarn, which is based on the LSVMB. Volume averaging method is applied to compute the global compliance or stiffness of plain-weave composite. The lower and upper impact bounds of the elastic constants of the composite are obtained from isostress and isostrain methods, respectively. The influence of FVF on the impact bounds of elastic constants of plain-weave composites is obtained by applying three values of yarn FVF into the estimation of elastic constants of plain-weave composites in stochastic waviness, scaling and twist cases, respectively.

From the results of numerical simulation, the impact bounds of elastic constants of plain-weave composites are affected by the variation of FVF of yarn. FVF influences the variation degrees of the impact bounds of elastic constants of plain-weave composites while the variation trends keep constant. When FVF increases from 0.5 to 0.9, the both impact bounds of elastic moduli decrease or are insensitive to the variations FVF in three cases. The both impact bounds of shear moduli increase or are insensitive to the variations FVF in three cases. The impact bounds of Poisson's ratios show different variation trends in three cases.

REFERENCE

[1] M. Olave, A. Vanaerschot, S.V. Lomov, D. Vandepitte, Internal geometry variability of two woven composites and related variability of the stiffness, Polymer Composites 33(8) (2012) 1335-1350.

[2] R. Rinaldi, M. Blacklock, H. Bale, M. Begley, B. Cox, Generating virtual textile composite specimens using statistical data from micro-computed tomography: 3D tow representations, J Mech Phys Solids 60 (2012) 1561-1581.

[3] H. Bale, M. Blacklock, M.R. Begley, D.B. Marshall, B.N. Cox, Characterizing Three-Dimensional Textile Ceramic Composites Using Synchrotron X-Ray Micro-Computed-Tomography, J. Am. Ceram. Soc. 95(1) (2012) 392-402.

[4] F. Gommer, K. Wedgwood, L. Brown, Stochastic reconstruction of filament paths in fibre bundles based on two-dimensional input data, Composites: Part A 76 (2015) 262-271.

[5] A. Vanaerschot, B.N. Cox, S.V. Lomov, D. Vandepitte, Stochastic framework for quantifying the geometrical variability of laminated textile composites using micro-computed tomography, Composites Part A 44 (2013) 122-131.

[6] A. Vanaerschot, B.N. Cox, S.V. Lomov, D. Vandepitte, Stochastic multi-scale modelling of textile composites based on internal geometry variability, Computers & Structures 122 (2013) 55-64.

[7] A. Vanaerschot, B.N. Cox, S.V. Lomov, D. Vandepitte, Experimentally validated stochastic geometry description for textile composite reinforcements, Composites Science and Technology 122 (2016) 122-129.

[8] H. Wang, Z.-w. Wang, Quantification of effects of stochastic feature parameters of yarn on elastic properties of plain-weave composite. Part 1: Theoretical modeling, Composites Part A 78 (2015) 84-94.

[9] H. Wang, Z.-w. Wang, A variable metric stochastic theory of textile composites with random geometric parameters of yarn cross-section, Composite Structures 126 (2015) 78-88.
[10] H. Wang, Z.-w. Wang, Quantification of effects of stochastic feature parameters of yarn on elastic properties of plain-weave composite – Part 2: Statistical predictions vs. mechanical experiments, Composites Part A 84 (2016) 147-157.
[11] C. Herakovich, Mechanics of fibrous composites, Wiley, New York, 1998.
[12] S.-K.B. Lee, Joon-Hyung; Hong, Soon Hyung, Effect of fiber geometry on the elastic constants of the plain woven fabric reinforced aluminum matrix composites, Materials Science and Engineering A 347 (2003) 13.
[13] K.-H.H. Tsai, Chung-Li; Chen, Wen-Liang; Chiu, Chang-Hsuan, A parallelogram spring model for predicting the effective elastic properties of 2 D braided composites, Composite Structures 83 (2008) 11.
[14] B. Cox, G. Flanagan, Handbook of Analytical Methods for Textile Composites, NASA Langley Technical Report Server, 1997.